

FERMI-LARGE AREA TELESCOPE OBSERVATIONS OF THE EXCEPTIONAL GAMMA-RAY OUTBURSTS OF 3C 273 IN 2009 SEPTEMBER

A. A. ABDO^{1,2}, M. ACKERMANN³, M. AJELLO³, L. BALDINI⁴, J. BALLE⁵, G. BARBIELLINI^{6,7}, D. BASTIERI^{8,9}, K. BECHTOL³, R. BELLAZZINI⁴, B. BERENJI³, R. D. BLANDFORD³, E. D. BLOOM³, E. BONAMENTE^{10,11}, A. W. BORGLAND³, A. BOUVIER³, J. BREGEON⁴, A. BREZ⁴, M. BRIGIDA^{12,13}, P. BRUEL¹⁴, T. H. BURNETT¹⁵, S. BUSON⁸, G. A. CALIANDRO¹⁶, R. A. CAMERON³, A. CANNON^{17,18}, P. A. CARAVEO¹⁹, S. CARRIGAN⁹, J. M. CASANDJIAN⁵, E. CAVAZZUTI²⁰, C. CECCHI^{10,11}, Ö. ÇELİK^{17,21,22}, E. CHARLES³, A. CHEKHTMAN^{1,23}, C. C. CHEUNG^{1,2}, J. CHIANG³, S. CIPRINI¹¹, R. CLAUS³, J. COHEN-TANUGI²⁴, J. CONRAD^{25,26,59}, L. COSTAMANTE³, C. D. DERMER¹, A. DE ANGELIS²⁷, F. DE PALMA^{12,13}, E. DO COUTO E SILVA³, P. S. DRELL³, R. DUBOIS³, D. DUMORA^{28,29}, C. FARNIER²⁴, C. FAVUZZI^{12,13}, S. J. FEGAN¹⁴, W. B. FOCKE³, M. FRAILIS^{27,30}, Y. FUKAZAWA³¹, S. FUNK³, P. FUSCO^{12,13}, F. GARGANO¹³, D. GASPARRINI²⁰, N. GEHRELS^{17,32,33}, S. GERMANI^{10,11}, N. GIGLIETTO^{12,13}, P. GIOMMI²⁰, F. GIORDANO^{12,13}, T. GLANZMAN³, G. GODFREY³, I. A. GRENIER⁵, M.-H. GRONDIN^{28,29}, S. GUIRIEC³⁴, M. HAYASHIDA³, E. HAYS¹⁷, A. B. HILL^{35,60}, D. HORAN¹⁴, R. E. HUGHES³⁶, G. JÓHANNESSEN³, A. S. JOHNSON³, W. N. JOHNSON¹, T. KAMAE³, H. KATAGIRI³¹, J. KATAOKA³⁷, N. KAWAI^{38,39}, J. KNÖDLSIEDER⁴⁰, M. KUSS⁴, J. LANDE³, S. LARSSON^{25,26}, L. LATRONICO⁴, M. LEMOINE-GOUMARD^{28,29}, M. LLENA GARDE^{25,26}, F. LONGO^{6,7}, F. LOPARCO^{12,13}, B. LOTT^{28,29}, M. N. LOVELLETTE¹, P. LUBRANO^{10,11}, G. M. MADEJSKI³, A. MAKEEV^{1,23}, O. MANSUTTI²⁷, E. MASSARO⁴¹, M. N. MAZZIOTTA¹³, W. MCCONVILLE^{17,33}, J. E. MCENERY^{17,33}, C. MEURER^{25,26}, P. F. MICHELSON³, W. MITTHUMSIRI³, T. MIZUNO³¹, A. A. MOISEEV^{21,33}, C. MONTE^{12,13}, M. E. MONZANI³, A. MORSELLI⁴², I. V. MOSKALENKO³, S. MURGIA³, P. L. NOLAN³, J. P. NORRIS⁴³, E. NUSS²⁴, T. OHSUGI⁴⁴, N. OMODEI³, E. ORLANDO⁴⁵, J. F. ORMES⁴³, D. PANEQUE³, J. H. PANETTA³, V. PELASSA²⁴, M. PEPE^{10,11}, M. PESCE-ROLLINS⁴, F. PRON²⁴, T. A. PORTER³, S. RAINÒ^{12,13}, R. RANDO^{8,9}, M. RAZZANO⁴, A. REIMER^{3,46}, O. REIMER^{3,46}, S. RITZ⁴⁷, A. Y. RODRIGUEZ¹⁶, R. W. ROMANI³, M. ROTH¹⁵, F. RYDE^{26,48}, H. F.-W. SADROZINSKI⁴⁷, A. SANDER³⁶, J. D. SCARGLE⁴⁹, T. L. SCHALK⁴⁷, C. SGRÒ⁴, E. J. SISKIND⁵⁰, P. D. SMITH³⁶, G. SPANDRE⁴, P. SPINELLI^{12,13}, J.-L. STARCK⁵, M. S. STRICKMAN¹, D. J. SUSON⁵¹, H. TAJIMA³, H. TAKAHASHI⁴⁴, T. TAKAHASHI⁵², T. TANAKA³, J. B. THAYER³, J. G. THAYER³, D. J. THOMPSON¹⁷, L. TIBALDO^{5,8,9,61}, D. F. TORRES^{16,53}, G. TOSTI^{10,11}, A. TRAMACERE^{3,54,55}, Y. UCHIYAMA³, T. L. USHER³, V. VASILEIOU^{21,22}, N. VILCHEZ⁴⁰, V. VITALE^{42,56}, A. P. WAITE³, P. WANG³, A. E. WEHRLE⁵⁷, B. L. WINER³⁶, K. S. WOOD¹, Z. YANG^{25,26}, T. YLINEN^{26,48,58}, AND M. ZIEGLER⁴⁷

¹ Space Science Division, Naval Research Laboratory, Washington, DC 20375, USA

² National Research Council Research Associate, National Academy of Sciences, Washington, DC 20001, USA

³ W. W. Hansen Experimental Physics Laboratory, Kavli Institute for Particle Astrophysics and Cosmology, Department of Physics and SLAC National Accelerator Laboratory, Stanford University, Stanford, CA 94305, USA

⁴ Istituto Nazionale di Fisica Nucleare, Sezione di Pisa, I-56127 Pisa, Italy

⁵ Laboratoire AIM, CEA-IRFU/CNRS/Université Paris Diderot, Service d'Astrophysique, CEA Saclay, 91191 Gif sur Yvette, France

⁶ Istituto Nazionale di Fisica Nucleare, Sezione di Trieste, I-34127 Trieste, Italy

⁷ Dipartimento di Fisica, Università di Trieste, I-34127 Trieste, Italy

⁸ Istituto Nazionale di Fisica Nucleare, Sezione di Padova, I-35131 Padova, Italy

⁹ Dipartimento di Fisica "G. Galilei," Università di Padova, I-35131 Padova, Italy

¹⁰ Istituto Nazionale di Fisica Nucleare, Sezione di Perugia, I-06123 Perugia, Italy; gino.tosti@pg.infn.it

¹¹ Dipartimento di Fisica, Università degli Studi di Perugia, I-06123 Perugia, Italy

¹² Dipartimento di Fisica "M. Merlin" dell'Università e del Politecnico di Bari, I-70126 Bari, Italy

¹³ Istituto Nazionale di Fisica Nucleare, Sezione di Bari, 70126 Bari, Italy

¹⁴ Laboratoire Leprince-Ringuet, École polytechnique, CNRS/IN2P3, Palaiseau, France

¹⁵ Department of Physics, University of Washington, Seattle, WA 98195-1560, USA

¹⁶ Institut de Ciències de l'Espai (IEEC-CSIC), Campus UAB, 08193 Barcelona, Spain

¹⁷ NASA Goddard Space Flight Center, Greenbelt, MD 20771, USA

¹⁸ University College Dublin, Belfield, Dublin 4, Ireland

¹⁹ INAF-Istituto di Astrofisica Spaziale e Fisica Cosmica, I-20133 Milano, Italy

²⁰ Agenzia Spaziale Italiana (ASI) Science Data Center, I-00044 Frascati (Roma), Italy

²¹ Center for Research and Exploration in Space Science and Technology (CRESSST) and NASA Goddard Space Flight Center, Greenbelt, MD 20771, USA

²² Department of Physics and Center for Space Sciences and Technology, University of Maryland Baltimore County, Baltimore, MD 21250, USA

²³ George Mason University, Fairfax, VA 22030, USA

²⁴ Laboratoire de Physique Théorique et Astroparticules, Université Montpellier 2, CNRS/IN2P3, Montpellier, France

²⁵ Department of Physics, Stockholm University, AlbaNova, SE-106 91 Stockholm, Sweden

²⁶ The Oskar Klein Centre for Cosmoparticle Physics, AlbaNova, SE-106 91 Stockholm, Sweden

²⁷ Dipartimento di Fisica, Università di Udine and Istituto Nazionale di Fisica Nucleare, Sezione di Trieste, Gruppo Collegato di Udine, I-33100 Udine, Italy

²⁸ CNRS/IN2P3, Centre d'Études Nucléaires Bordeaux Gradignan, UMR 5797, Gradignan 33175, France

²⁹ Université de Bordeaux, Centre d'Études Nucléaires Bordeaux Gradignan, UMR 5797, Gradignan 33175, France

³⁰ Osservatorio Astronomico di Trieste, Istituto Nazionale di Astrofisica, I-34143 Trieste, Italy

³¹ Department of Physical Sciences, Hiroshima University, Higashi-Hiroshima, Hiroshima 739-8526, Japan

³² Department of Astronomy and Astrophysics, Pennsylvania State University, University Park, PA 16802, USA

³³ Department of Physics and Department of Astronomy, University of Maryland, College Park, MD 20742, USA

³⁴ Center for Space Plasma and Aeronomic Research (CSPAR), University of Alabama in Huntsville, Huntsville, AL 35899, USA

³⁵ Université Joseph Fourier-Grenoble 1/CNRS, laboratoire d'Astrophysique de Grenoble (LAOG), UMR 5571, BP 53, 38041 Grenoble Cedex 09, France

³⁶ Department of Physics, Center for Cosmology and Astro-Particle Physics, The Ohio State University, Columbus, OH 43210, USA

³⁷ Research Institute for Science and Engineering, Waseda University, 3-4-1 Okubo, Shinjuku, Tokyo 169-8555, Japan

³⁸ Department of Physics, Tokyo Institute of Technology, Meguro City, Tokyo 152-8551, Japan

³⁹ Cosmic Radiation Laboratory, Institute of Physical and Chemical Research (RIKEN), Wako, Saitama 351-0198, Japan

⁴⁰ Centre d'Étude Spatiale des Rayonnements, CNRS/UPS, BP 44346, F-30128 Toulouse Cedex 4, France

⁴¹ Dipartimento di Fisica, Università di Roma "La Sapienza," I-00185 Roma, Italy; enrico.massaro@uniroma1.it

⁴² Istituto Nazionale di Fisica Nucleare, Sezione di Roma "Tor Vergata," I-00133 Roma, Italy

⁴³ Department of Physics and Astronomy, University of Denver, Denver, CO 80208, USA

⁴⁴ Hiroshima Astrophysical Science Center, Hiroshima University, Higashi-Hiroshima, Hiroshima 739-8526, Japan

⁴⁵ Max-Planck Institut für extraterrestrische Physik, 85748 Garching, Germany

⁴⁶ Institut für Astro- und Teilchenphysik and Institut für Theoretische Physik, Leopold-Franzens-Universität Innsbruck, A-6020 Innsbruck, Austria

⁴⁷ Santa Cruz Institute for Particle Physics, Department of Physics and Department of Astronomy and Astrophysics, University of California at Santa Cruz, Santa Cruz, CA 95064, USA

⁴⁸ Department of Physics, Royal Institute of Technology (KTH), AlbaNova, SE-106 91 Stockholm, Sweden

⁴⁹ Space Sciences Division, NASA Ames Research Center, Moffett Field, CA 94035-1000, USA

⁵⁰ NYCB Real-Time Computing Inc., Lattingtown, NY 11560-1025, USA

⁵¹ Department of Chemistry and Physics, Purdue University Calumet, Hammond, IN 46323-2094, USA

⁵² Institute of Space and Astronautical Science, JAXA, 3-1-1 Yoshinodai, Sagami-hara, Kanagawa 229-8510, Japan

⁵³ Institut de Recerca i Estudis Avançats (ICREA), Barcelona, Spain

⁵⁴ Consorzio Interuniversitario per la Fisica Spaziale (CIFS), I-10133 Torino, Italy

⁵⁵ INTEGRAL Science Data Centre, CH-1290 Versoix, Switzerland

⁵⁶ Dipartimento di Fisica, Università di Roma "Tor Vergata," I-00133 Roma, Italy

⁵⁷ Space Science Institute, Boulder, CO 80301, USA

⁵⁸ School of Pure and Applied Natural Sciences, University of Kalmar, SE-391 82 Kalmar, Sweden

Received 2010 January 29; accepted 2010 March 15; published 2010 April 5

ABSTRACT

We present the light curves and spectral data of two exceptionally luminous gamma-ray outbursts observed by the Large Area Telescope experiment on board the *Fermi Gamma-ray Space Telescope* from 3C 273 in 2009 September. During these flares, having a duration of a few days, the source reached its highest γ -ray flux ever measured. This allowed us to study, in some details, their spectral and temporal structures. The rise and the decay are asymmetric on timescales of 6 hr, and the spectral index was significantly harder during the flares than during the preceding 11 months. We also found that short, very intense flares put out the same time-integrated energy as long, less intense flares like that observed in 2009 August.

Key words: gamma rays: galaxies – quasars: individual (3C 273)

Online-only material: color figure

1. INTRODUCTION

The Large Area Telescope (LAT) experiment, on board the *Fermi Gamma-ray Space Telescope* satellite, observes the entire sky, in the 0.02 to >300 GeV band, once every ~ 3 hr. It is providing the first collection of well-sampled gamma-ray light curves of several blazars useful to study their variability on timescales from day to several months (see, e.g., Abdo et al. 2010c). Daily light curves can be obtained for several blazars, and for those exceptionally bright it is possible to observe significant occasional variations on timescales shorter than a day. We have now observed such events in 3C 273, the nearest quasar.

3C 273, the first quasar discovered by Schmidt (1963) and the first extragalactic source detected by *COS-B* in the gamma-ray band (Swanenburg et al. 1978), is one of the most extensively studied active galactic nucleus (AGN) across the entire electromagnetic spectrum. It is classified as a flat spectrum radio quasar (FSRQ) and has a redshift $z = 0.158$ (see, e.g., Strauss et al. 1992). It was observed by EGRET (3EG J1229+0210 in Hartman et al. 1999) at an average flux of 0.18×10^{-6} photons $\text{cm}^{-2} \text{s}^{-1}$ with a peak flux of 1.27×10^{-6} photons $\text{cm}^{-2} \text{s}^{-1}$ (Nandikotkur et al. 2007). Despite the huge amount of data collected till now (see for instance Soldi et al. 2008), its behavior is still surprising and raises new challenges for physical models. It was detected by the LAT experiment since the beginning of

the observation in 2008 (Marelli 2008) and is identified with the gamma-ray source 1FGL J1229.1+0203 in the first *Fermi-LAT* catalog (Abdo et al. 2010a). For about one year, its behavior was characterized by a rather stable flux of $\sim 0.3 \times 10^{-6}$ photons $\text{cm}^{-2} \text{s}^{-1}$, with some flares superposed reaching peak level higher by about an order of magnitude.

Beginning at the end of 2009 July, 3C 273 started a brightening phase during which some very bright outbursts were observed. The first event lasted about 10 days in 2009 August (Bastieri 2009) and was characterized by fast rise and decay times (< 1 day) and a relatively stable "plateau." In contrast, the second and third outbursts were sharply peaked from 2009 September 15 to 17 and from 2009 September 20 to 23 (Hill 2009), when 3C 273 reached a peak photon flux above 10^{-5} photons $\text{cm}^{-2} \text{s}^{-1}$. Before the very recent (2009 December) flare observed in 3C 454.3 (Escande & Tanaka 2009; Striani et al. 2009), it was, therefore, the brightest extragalactic source, non gamma-ray burst, observed by *Fermi*. EGRET detected only a few blazars (e.g., 3C 279 and PKS 1622–297) with a flux above 10^{-5} photons $\text{cm}^{-2} \text{s}^{-1}$.

Thanks to the high flux, it was possible to obtain light curves with a good signal-to-noise ratio with a time binning of only 6 hr (corresponding to two scans of sky) and therefore we can describe the evolution of this outburst with a level of detail never reached before. In this Letter, we present the results of the LAT observations.

2. OBSERVATIONS WITH THE LAT

The *Fermi-LAT* is a pair-conversion γ -ray telescope sensitive to photon energies from 20 MeV to >300 GeV. It is made of a

⁵⁹ Royal Swedish Academy of Sciences Research Fellow, funded by a grant from the K. A. Wallenberg Foundation.

⁶⁰ Funded by contract ERC-StG-200911 from the European Community.

⁶¹ Partially supported by the International Doctorate on Astroparticle Physics (IDAPP) program.

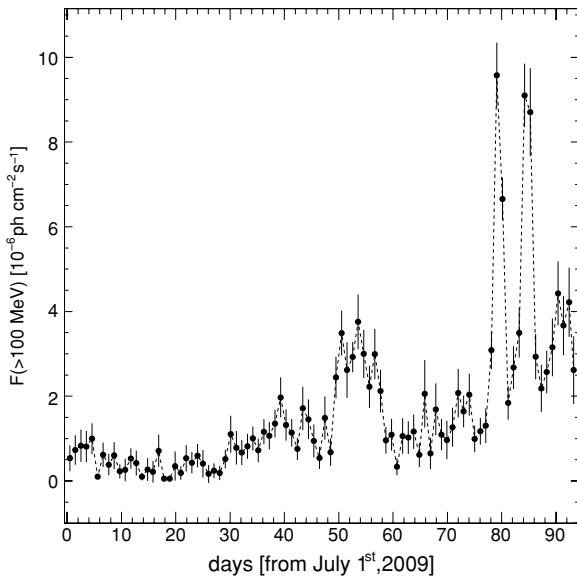


Figure 1. 1-day gamma-ray light curve of 3C 273 in the period from 2009 July 1 (MJD=55013) to September 30 (MJD=55104).

tracker (composed of two sections, front and back, with different capabilities), a calorimeter, and an anticoincidence system to reject the charged-particle background. The LAT has a large peak effective area ($\sim 8000 \text{ cm}^2$ for 1 GeV photons in the event class considered here), viewing ~ 2.4 sr of the full sky with excellent angular resolution (68% containment radius better than $\sim 1^\circ$ at $E = 1$ GeV). A full description of the LAT instrument and its performance are reported in Atwood et al. (2009). During the first year, the telescope operated in sky-survey mode, observing the whole sky every 3 hr.

Only photons in “diffuse” class with energies greater than 100 MeV were considered in this analysis. We kept only events with reconstructed zenith angle $< 105^\circ$ in order to reduce the bright γ -ray albedo from the Earth. In addition, we excluded the time intervals when the rocking angle was more than 52° and when the *Fermi* satellite was within the South Atlantic Anomaly. The standard *Fermi-LAT Science Tools* software package⁶² (version v9r15p6) was used with the P6 V3 set of instrument response functions. This version of the Science Tools takes into account the correction for the residual acceptance variation with count rate. Light curves were produced in 1-day (see Figure 1) bins over the period 2009 July–September, and in 12- and 6-hr (see Figure 2) bins in 2009 September. For each time bin, the flux, photon index, and test statistic of 3C 273 were determined, in the energy range 0.1–100 GeV. We analyzed a Region of Interest (RoI) of 12° in radius, centered at the position of the γ -ray source associated with 3C 273, using the maximum-likelihood algorithm implemented in *gllike*. In the RoI analysis, the sources were modeled as simple power law ($F = KE^{-\Gamma}$). The source model parameters are free for all point sources within 5° of 3C 273 (extracted from the LAT 1FGL catalog,⁶³ see Abdo et al. 2010a). In the RoI model, we also included all sources from 5° to 17° of 3C 273, with their model parameters fixed to their catalog values.

The Galactic diffuse background model included in the RoI analysis is the currently recommended version (*gll_iem_v02*), publicly released through the *Fermi* Science Support Center. The

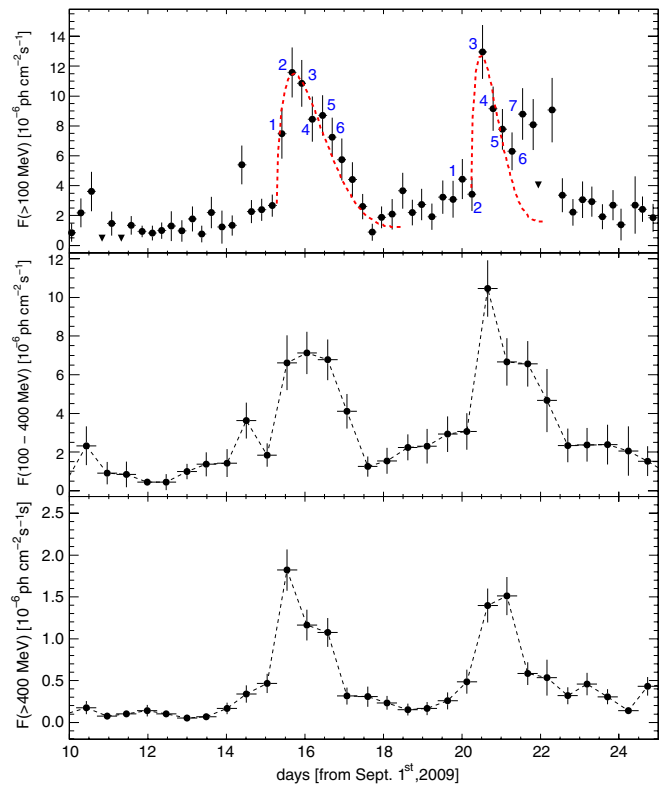


Figure 2. Upper panel shows the 6-hr light curve of 3C 273 during the large outbursts in 2009 September. The points marked with triangles indicate upper limits. The middle and lower panels show 12-hr light curves of 3C 273 during the large outburst in 2009 September in the energy range 0.1–0.4 GeV and at energies higher than 0.4 GeV, respectively.

(A color version of this figure is available in the online journal.)

isotropic background (including the γ -ray diffuse and residual instrumental backgrounds) model was derived from an overall fit of the diffuse component over the $|b| > 30^\circ$ sky. A detailed documentation of the Galactic diffuse model and corresponding isotropic spectrum is available from the *Fermi* Science Support Center.⁶⁴

All errors reported in the figures or quoted in the text are 1σ statistical errors. The estimated systematic uncertainty on the flux is 10% at 100 MeV, 5% at 500 MeV, and 20% at 10 GeV.

3. TIME EVOLUTION OF THE OUTBURSTS

The light curve of the very large outburst for photon energies above 0.1 GeV and with a time binning of 6 hr is plotted in the upper panel of Figure 2. The outburst’s structure consists of two main flares, each one having a total duration of about a couple of days and peak flux of $\sim 1.2 \times 10^{-5}$ photons $\text{cm}^{-2} \text{s}^{-1}$. The first flare shows a nice smooth time profile, suggesting that it is well resolved; the second flare, after a first short peak, shows a series of high bins that can be indication either of substructures or of a long decay tail.

The profile of the first flare is clearly asymmetric with a fast rise of the duration of about 12 hr, and a longer decay of about 36 hr. We modeled its evolution by means of the law of the following formula:

$$F(t) = F_0 + K(1 + t/T_1)^\alpha (1 - t/T_2)^\beta, \quad (1)$$

that is derived from the statistical Beta distribution (see for instance Johnson et al. 1994) and is also known as a Pearson

⁶² <http://fermi.gsfc.nasa.gov/ssc/data/analysis/documentation/Cicerone/>

⁶³ http://fermi.gsfc.nasa.gov/ssc/data/access/lat/1yr_catalog/

⁶⁴ <http://fermi.gsfc.nasa.gov/ssc/data/access/lat/BackgroundModels.html>

curve of Type I (Smart 1958). It is defined in the interval $(-T_1, T_2)$ (a shift of the time origin is necessary for the fitting to data) and $F(-T_1) = F(T_2) = F_0$ at the extremes of that interval, then it is well suitable to model burst of finite durations. This function can be used to model the time evolution of flares, having either convex or concave rising and decaying profiles. It is more general than the one applied in Abdo et al. (2010c), which presented and analyzed the gamma-ray light curves of the 106 high-confidence *Fermi*-LAT Bright AGN Sample (Abdo et al. 2009) obtained during the first 11 months of the *Fermi* survey. The flares of the 10 brightest blazars were modeled by a law, defined as the inverse of the sum of two exponentials, to quantify the symmetry and duration of individual episodes. The total duration of the flare is given by $T_1 + T_2$, while we can easily measure its asymmetry by evaluating the difference between the decay and the rise time divided by their sum, which gives

$$\xi = \frac{\beta - \alpha}{\alpha + \beta}. \quad (2)$$

For the first burst, we find $T_1 = 18$ hr, $T_2 = 60$ hr, $\alpha = 0.5$, $\beta = 3.2$, and $\xi = 0.73$. The complex structure of the second flare makes the fitting of Equation (1) very hard; however, considering only the first five data points we obtained a reasonable fit with $T_1 = 12$ hr and $T_2 = 33$ hr and using the same values of α and β (see Figure 2). The resulting χ^2 are smaller than unity in both cases. This result differs from those of the other six and much longer bursts observed by the LAT till 2009 July (Abdo et al. 2010c). These flares had durations in the range from 8 to 58 days and were generally nearly symmetric, and their ξ values were usually in the interval $(-0.38, -0.22)$, with the only exception being the longest one for which ξ was -0.72 . Although the function used in the flare analysis of 3C 273 presented by Abdo et al. (2010c) was not that of Equation (1), the quantity ξ was the same and depends only on the time elapsed between the peak and the starting and ending points of the flare. The highest brightness level reached in those flares, however, was much lower than that of the 2009 September outbursts: the typical flux of 3C 273 was around 3×10^{-7} photons $\text{cm}^{-2} \text{s}^{-1}$ with peak values during the flares of 2.5×10^{-6} photons $\text{cm}^{-2} \text{s}^{-1}$. Comparable fluxes were measured by the GRID instrument, on board the *AGILE* satellite, from 2007 December to 2008 January (Pacciani et al. 2009).

It is interesting to evaluate the rising and decay flux rates of the two flares. The rises were both very short, and the estimates of the corresponding flux rates at about half of the rising branch are 1.3×10^{-8} photons $\text{cm}^{-2} \text{s}^{-1} \text{hr}^{-1}$ and 2.0×10^{-8} photons $\text{cm}^{-2} \text{s}^{-1} \text{hr}^{-1}$ for the first and second flare, respectively. The decays evolved on longer timescale with flux rates of 0.3×10^{-8} photons $\text{cm}^{-2} \text{s}^{-1} \text{hr}^{-1}$ and 0.5×10^{-8} photons $\text{cm}^{-2} \text{s}^{-1} \text{hr}^{-1}$.

The very fast variability, however, does not correspond to an increase of the time-integrated energy output from the source, at least when they are compared with that of August. In fact, the fluence of this flare, estimated by the integration of the best fit model over the duration of the event, is 2.06 photons cm^{-2} , while those of the other and higher two flares are 1.59 and 1.05 photons cm^{-2} . The last value is that of the main peak and increases by about 0.5 photons cm^{-2} when the three last bins are included.

A comparison of the power density spectrum (PDS) of the 90 day flaring episode in Figure 1, with one computed for the first 11 months of data, did not show any substantial difference

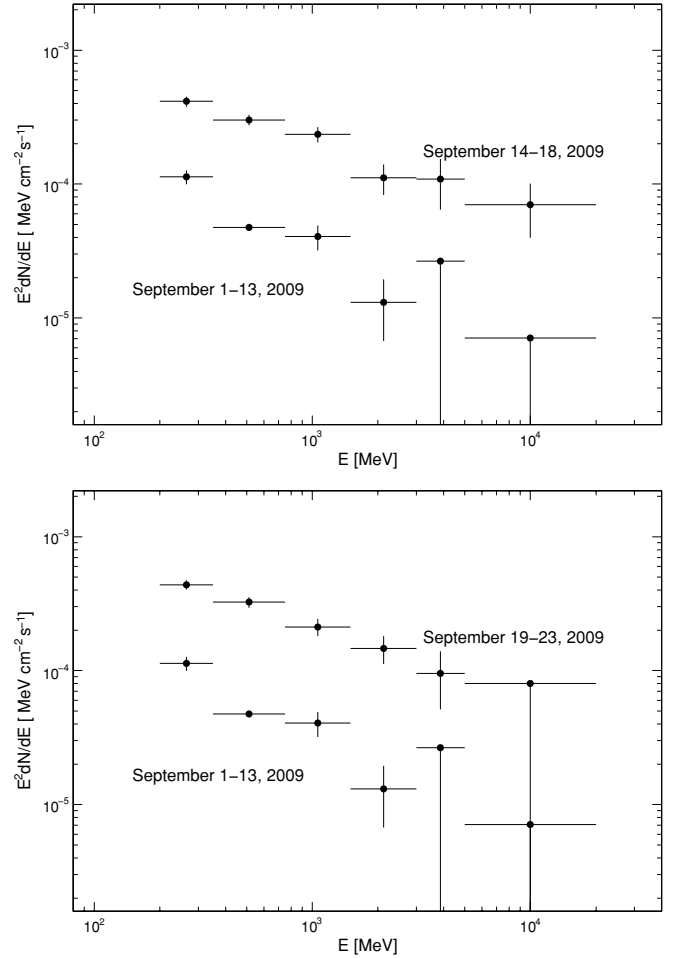


Figure 3. Spectral energy distributions (SEDs) of 3C 273 in the quiescent phase and during the two September outbursts.

in shape, although the flare PDS had slightly more power at frequencies $>0.1 \text{ days}^{-1}$. The fractional variability (rms/flux) for frequencies above 0.01 days^{-1} in the PDS was, however, three times higher during the flaring episode than during the initial 11 months (0.99 and 0.32, respectively). In other words, the source was more variable during the flaring period of July–September than in the preceding 11 months.

4. SPECTRAL BEHAVIOR

Figure 3 shows the spectral energy distribution, in the band 100 MeV–20 GeV, of 3C 273 during the September outbursts. The spectra were obtained fitting a power-law model over seven energy bins, with the spectral index kept fixed at the values obtained by the fit in the entire energy range over the same time interval.

We also computed the spectra of 3C 273 integrating over the two weeks from September 1 to 13, during the quiescent phase preceding the September events, and found that it is well described by a power law with photon index $\Gamma = 2.86 \pm 0.02$ (see Figure 3). The spectra of the two major outbursts integrated over the time intervals from 2009 September 14 to 18 and from September 19 to 22 showed flatter slopes $\Gamma = 2.43 \pm 0.01$ and 2.52 ± 0.01 , respectively, confirming that the average spectrum during the outbursts was significantly but moderately harder than in the quiescent state. As reported in Abdo et al. (2010d), the spectrum of 3C 273 integrated over the 6 months showed

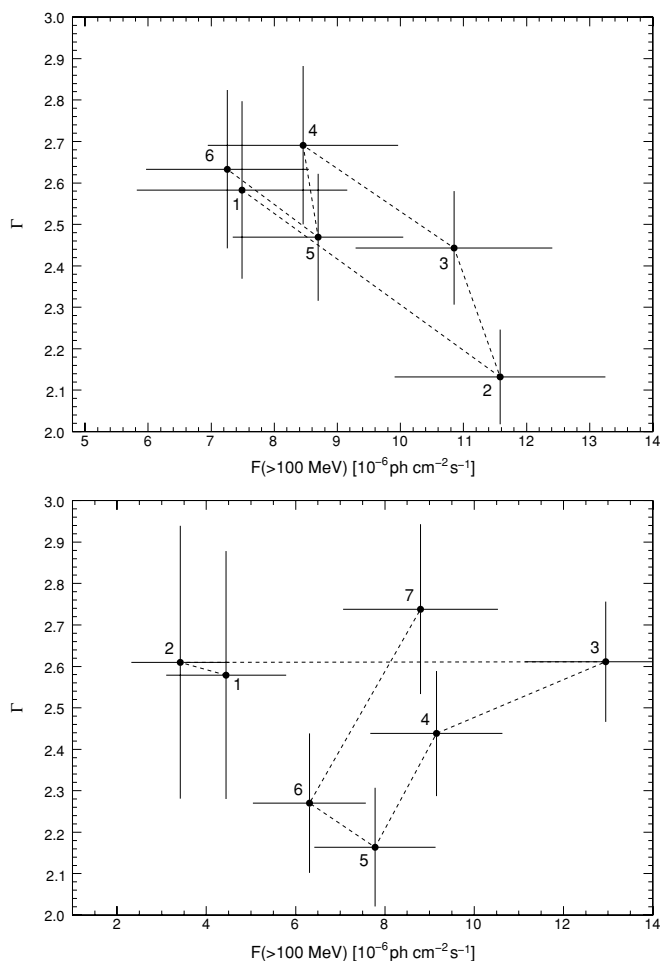


Figure 4. This figure shows the variation of Γ during the large flares observed in 2009 September 15–16 (upper panel) and 2009 September 19–21 (lower panel). In the upper panel, the point having the label (1) corresponds to 2009 September 15.30, the other points correspond to successive 6-hr time bins (see also Figure 2, upper panel). In the lower panel, the point having the label (1) corresponds to 2009 September 19.88, the other points correspond to successive 6-hr time bins (see also Figure 2, upper panel).

a significant break around 1.5 GeV. Our spectra of the source integrated over shorter periods of time do not provide indication for a curvature in the spectra.

It is worth noting that, so far, the spectral change with respect to flux has been observed to be very moderate in other FSRQs (e.g., 3C 454.3; see Abdo et al. 2010d), even during large flares. An interesting indication of a possible spectral evolution during the major bursts of 3C 273 can be obtained by the light curves in two energy bands. The central and lower panel of Figure 2 shows the outburst evolution in the energy ranges (0.1–0.4) GeV and above 0.4 GeV with a time bin width of 12 hr. Despite the large differences in the photon fluxes, we see that the profile of the peaks are rather similar with an indication that above 0.4 GeV peaks are sharper and with shorter decay times.

Time-resolved spectral indices show possible spectral changes during the two major bursts as illustrated by the Γ versus flux plots in Figure 4. The start and end ranges of the data used to demarcate the two flares were defined as the time intervals containing the 90% of the total flux, starting when the 10% level was measured. A “counterclockwise” loop is observed during the first flare. The spectrum becomes steeper in the declining phase and harder in the brightening phase. During the second flare, the spectral index changes following a

path that is essentially “clockwise.” In this case, the brightening phase was very rapid and the spectral index remained constant, after the flare peak the spectrum becomes harder and then softer again. A clockwise loop can indicate that during the first flare the flux started to increase at low energy and then propagate to high energy, the inverse could have happened during the second flare.

5. DISCUSSION

The large outburst of 3C 273 observed by *Fermi* in 2009 September revealed that blazars can reach very high brightness levels for quite short time intervals of 1–10 days.

The fluences of these events, however, are comparable to that of longer but less intense flares. We measured significant variations of the flux over timescales as short as 6 hr, which occurred with only a mild change of the spectral shape.

In contrast to previous low-intensity flares (Abdo et al. 2010c), the very strong events of September have light curves characterized by decay times longer than the rise time. Light curves at different energies provide some indication, in particular, for the second flare, that the decay rate above 0.4 GeV is shorter than that below. The most natural interpretation of this difference is that it is due to the radiative cooling of the high-energy electrons responsible for the γ -ray emission. We can therefore estimate that this time, as observed in the Earth’s frame, is of the order of 0.5–1 day. Such short lifetimes explain why longer flares are generally symmetric. In fact, it is possible that they are structured in a series of short subflares with typical durations of 2–3 days, much shorter than the total flare length. The apparent rise and decay times of long events are then likely due to the superposition of quite shorter flares and any information on the radiative lifetimes is practically lost.

In 2009 September, the apparent position of 3C 273 was rather close to the Sun, making it was practically impossible to perform observations in other frequency ranges. Therefore, we do not have data to study the evolution of the broadband SED. The typical SEDs of FSRQs (Abdo et al. 2010b) peak at rather low γ -ray energies, around 0.1 GeV and frequently lower. In the case of 3C 273, which was the most significant AGN detected by COMPTEL in the 1–30 MeV range, the peak of the inverse Compton component was in the range 1–10 MeV (Collmar et al. 2000). Our data show that the photon index was always steeper than 2, and this indicates that the peak energy remained below 100 MeV also during the flares.

γ -ray activity has been found to be related to changes of the blazars’ radio structure observed with very long baseline interferometry (VLBI). In this respect, 3C 273 is one of the most interesting sources because of the flux and of the low redshift that allows a fine spatial resolution. Jorstad et al. (2001), on the basis of a large data set at 22 and 43 GHz, found an association between the ejection of superluminal radio knots and high states of γ -ray luminosity in ten blazars in EGRET observations, including 3C 273. They concluded that both the radio and high-energy events are originating from the same shocked region of a relativistic jet. Similar correspondences were already reported for the two much more distant FSRQs S5 0836+710 (Otterbein et al. 1998) and PKS 0528+134 (Britzen et al. 1999).

More recent results on the MOJAVE Very Long Baseline Array (VLBA) sample and *Fermi*-LAT observations (Lister et al. 2009; Savolainen et al. 2009) provided evidence that γ -ray loud blazars have a Doppler factor higher than non-LAT-detected sources. A detailed plot of the kinematics of the

various components in the radio jet of 3C 273 can be found in Lister et al. (2009b): the resulting mean superluminal velocity is $\beta_{\text{app}} = 13.4$ with an estimated Doppler factor $\delta = 16.8$.

It will be very interesting to verify if the exceptional outbursts of 2009 September will or will not be associated with the ejection of new superluminal knots, possibly with even higher velocity and Doppler factor. Moreover, the discovery of a possible connection between the peak intensity and rise time of the γ -ray outbursts with the VLBI parameters can be very useful to constrain the modeling and the energetics of perturbations in the jet.

The *Fermi*-LAT Collaboration acknowledges generous ongoing support from a number of agencies and institutes that have supported both the development and the operation of the LAT, as well as scientific data analysis. These include the National Aeronautics and Space Administration and the Department of Energy in the United States, the Commissariat à l'Énergie Atomique and, the Centre National de la Recherche Scientifique/Institut National de Physique Nucléaire et de Physique des Particules in France, the Agenzia Spaziale Italiana and, the Istituto Nazionale di Fisica Nucleare in Italy, the Ministry of Education, Culture, Sports, Science and Technology (MEXT), High Energy Accelerator Research Organization (KEK), and Japan Aerospace Exploration Agency (JAXA) in Japan, and the K. A. Wallenberg Foundation, the Swedish Research Council, and the Swedish National Space Board in Sweden. Additional support for science analysis during the operations phase is gratefully acknowledged from the Istituto Nazionale di Astrofisica in Italy and the Centre National d'Études Spatiales.

Facility: *Fermi* ()

REFERENCES

- Abdo, A. A., et al. 2009, *ApJ*, **700**, 597
 Abdo, A. A., et al. 2010a, submitted (arXiv:1002.2280)
 Abdo, A. A., et al. 2010b, submitted (arXiv:0912.2040)
 Abdo, A. A., et al. 2010c, submitted
 Abdo, A. A., et al. 2010d, *ApJ*, **710**, 1271
 Atwood, W. B., et al. 2009, *ApJ*, **697**, 1071
 Bastieri, D. 2009, *ATel*, **2168**, 1
 Britzen, S., Witzel, A., Krichbaum, T. P., Qian, S. J., & Campbell, R. M. 1999, *A&A*, **341**, 418
 Collmar, W., et al. 2000, *A&A*, **354**, 513
 Escande, L., & Tanaka, Y. T. 2009, *ATel*, **2328**, 1
 Hartman, R. C., et al. 1999, *ApJS*, **123**, 79
 Hill, A. B. 2009, *ATel*, **2200**, 1
 Johnson, N. L., Kotz, S., & Balakrishnan, N. 1994, *Continuous Univariate Distributions* (New York: Wiley)
 Jorstad, S. G., Marscher, A. P., Mattox, J. R., Wehrle, A. E., Bloom, S. D., & Yurchenko, A. V. 2001, *ApJS*, **134**, 181
 Lister, M. L., Homan, D. C., Kadler, M., Kellermann, K. I., Kovalev, Y. Y., Ros, E., Savolainen, T., & Zensus, J. 2009, *ApJ*, **696**, 22
 Lister, M. L., et al. 2009b, *AJ*, **138**, 1874
 Marelli, M. 2008, *ATel*, **1707**, 1
 Nandikotkur, G., Jahoda, K. M., Hartman, R. C., Mukherjee, R., Sreekumar, P., Böttcher, M., Sambruna, R. M., & Swank, J. H. 2007, *ApJ*, **657**, 706
 Otterbein, K., Krichbaum, T. P., Kraus, A., Lobanov, A. P., Witzel, A., Wagner, S. J., & Zensus, J. A. 1998, *A&A*, **334**, 489
 Pacciani, L., et al. 2009, *A&A*, **494**, 49
 Savolainen, T., Homan, D. C., Hovatta, T., Kadler, M., Kovalev, Y. Y., Lister, M. L., Ros, E., & Zensus, J. A. 2009, *A&A*, submitted (arXiv:0911.4924)
 Schmidt, M. 1963, *Nature*, **197**, 1040
 Smart, W. M. 1958, *Combination of Observations* (Cambridge: Cambridge Univ. Press)
 Soldi, S., et al. 2008, *A&A*, **486**, 411
 Strauss, M. A., Huchra, J. P., Davis, M., Yahil, A., Fisher, K. B., & Tonry, J. 1992, *ApJS*, **83**, 29
 Striani, E., et al. 2009, *ATel*, **2322**, 1
 Swanenburg, B. N., et al. 1978, *Nature*, **275**, 298